Supporting Information

Morphology control synthesis of $[Mo_3S_{13}]^{2-}$/Co-MOF-74 composite catalysts and their application in the oxygen evolution reaction

Jianxia Gu[a]*, Jingting He[b], Haiyan Zheng[b], Chunyi Sun[b]*

[a]*Department of chemistry, Xinzhou Normal University, Xinzhou, Shanxi, China*

[b]*National & Local United Engineering Laboratory for Power Batteries, Department of Chemistry, Northeast Normal University, Changchun, Jilin, China.*

Figures

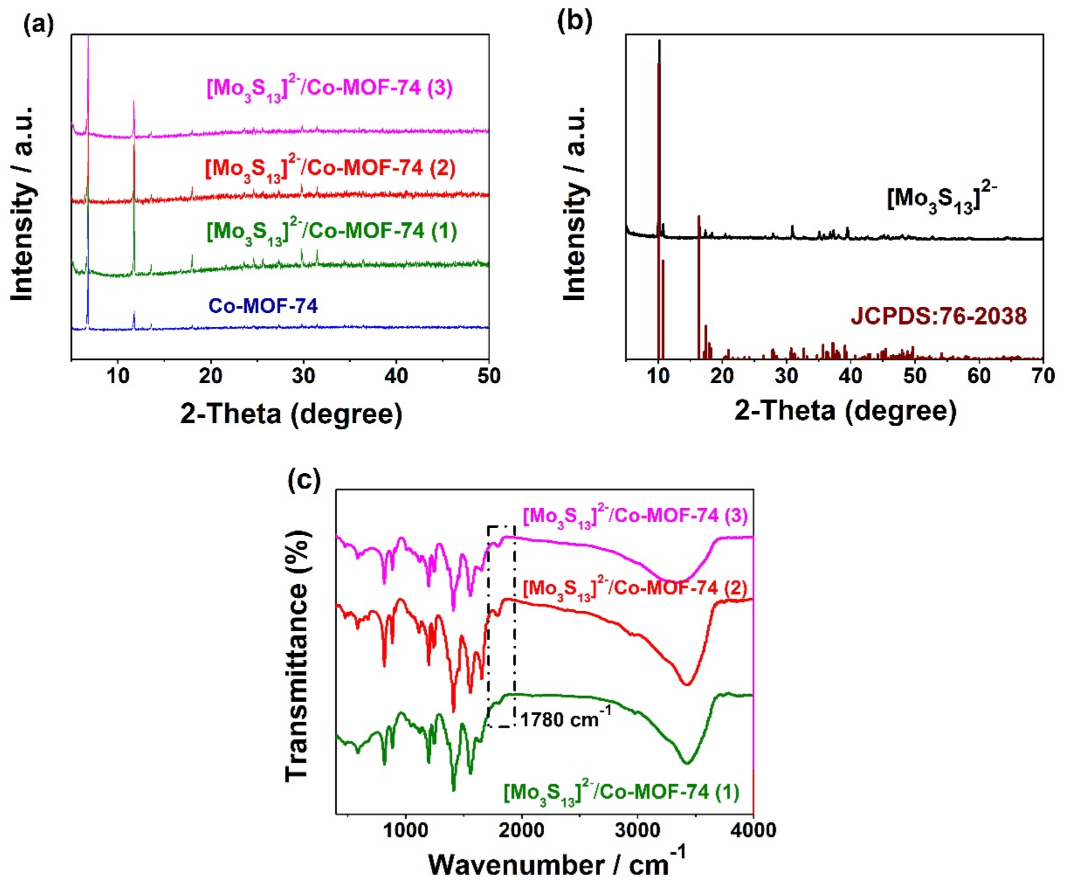

Fig. S1 (a) X-ray diffraction patterns (XRD) of Co-MOF-74, Co-MOF-74/$[Mo_3S_{13}]^{2-}$ **(1)**, Co-MOF-74/$[Mo_3S_{13}]^{2-}$ **(2)**, and Co-MOF-74/$[Mo_3S_{13}]^{2-}$ **(3)**. (b) XRD patterns of $[Mo_3S_{13}]^{2-}$ and a standard card of $(NH_4)_2Mo_3S_{13}\cdot nH_2O$ (JCPDS 76-2038). (c) Fourier transformed infrared (FT-IR) spectra of Co-MOF-74/$[Mo_3S_{13}]^{2-}$ **(1)**, Co-MOF-74/$[Mo_3S_{13}]^{2-}$ **(2)**, and Co-MOF-74/$[Mo_3S_{13}]^{2-}$ **(3)**.

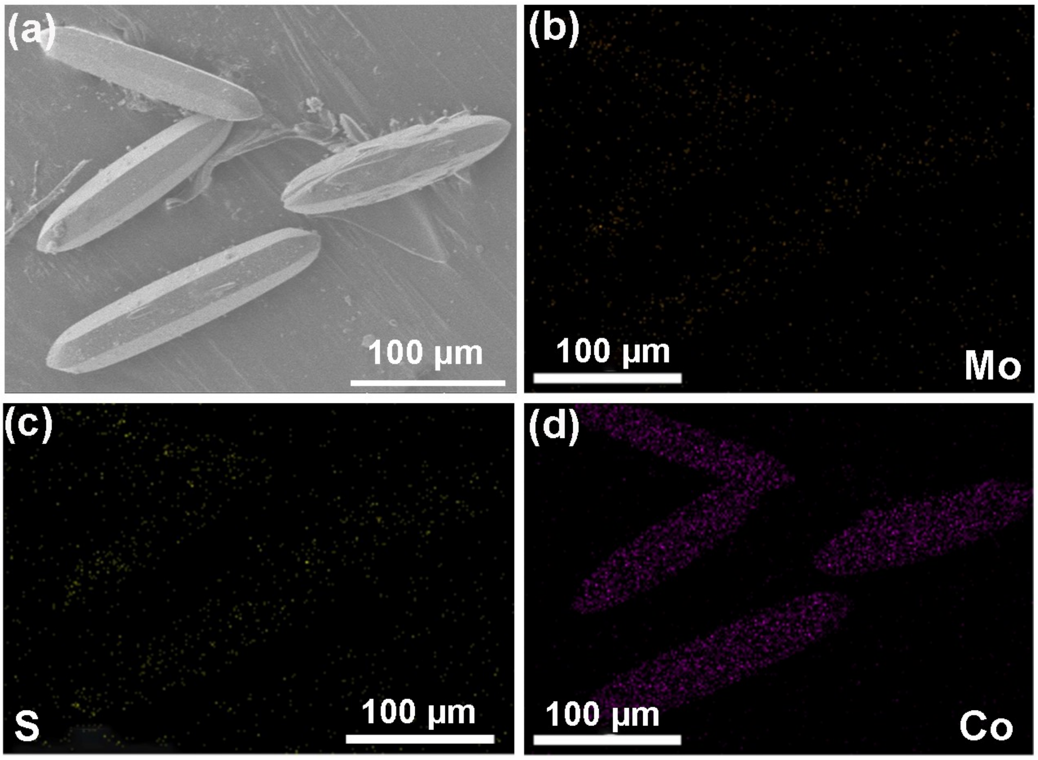

Fig. S2 (a-d) The EDS elemental mapping for $[Mo_3S_{13}]^{2-}$/Co-MOF-74 **(2)**.

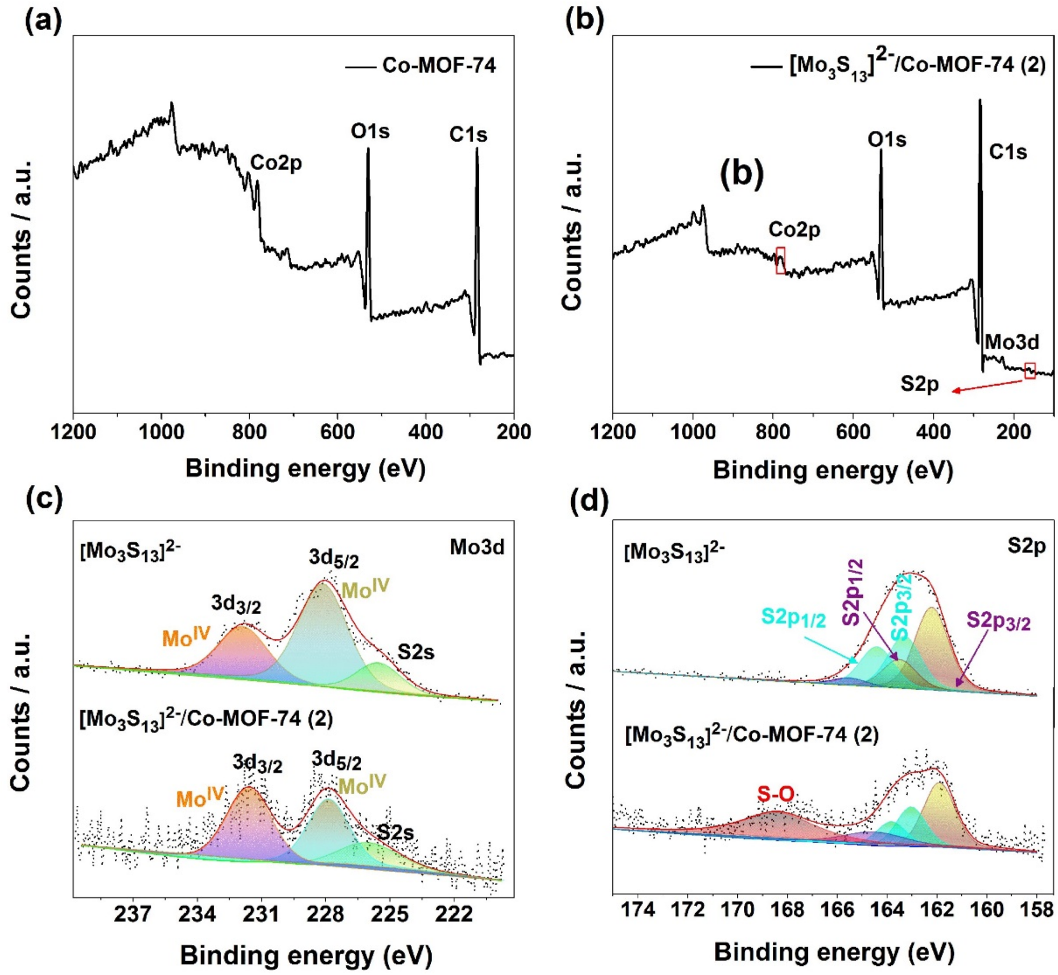

Fig. S3 The survey X-ray photoelectron spectroscopy (XPS) spectra of Co-MOF-74 (a) and $[Mo_3S_{13}]^{2-}$/Co-MOF-74 **(2)** (b). The high-resolution XPS spectra of Mo 3d (c) and S 2p (d) in the $[Mo_3S_{13}]^{2-}$ and $[Mo_3S_{13}]^{2-}$/Co-MOF-74 **(2)**.

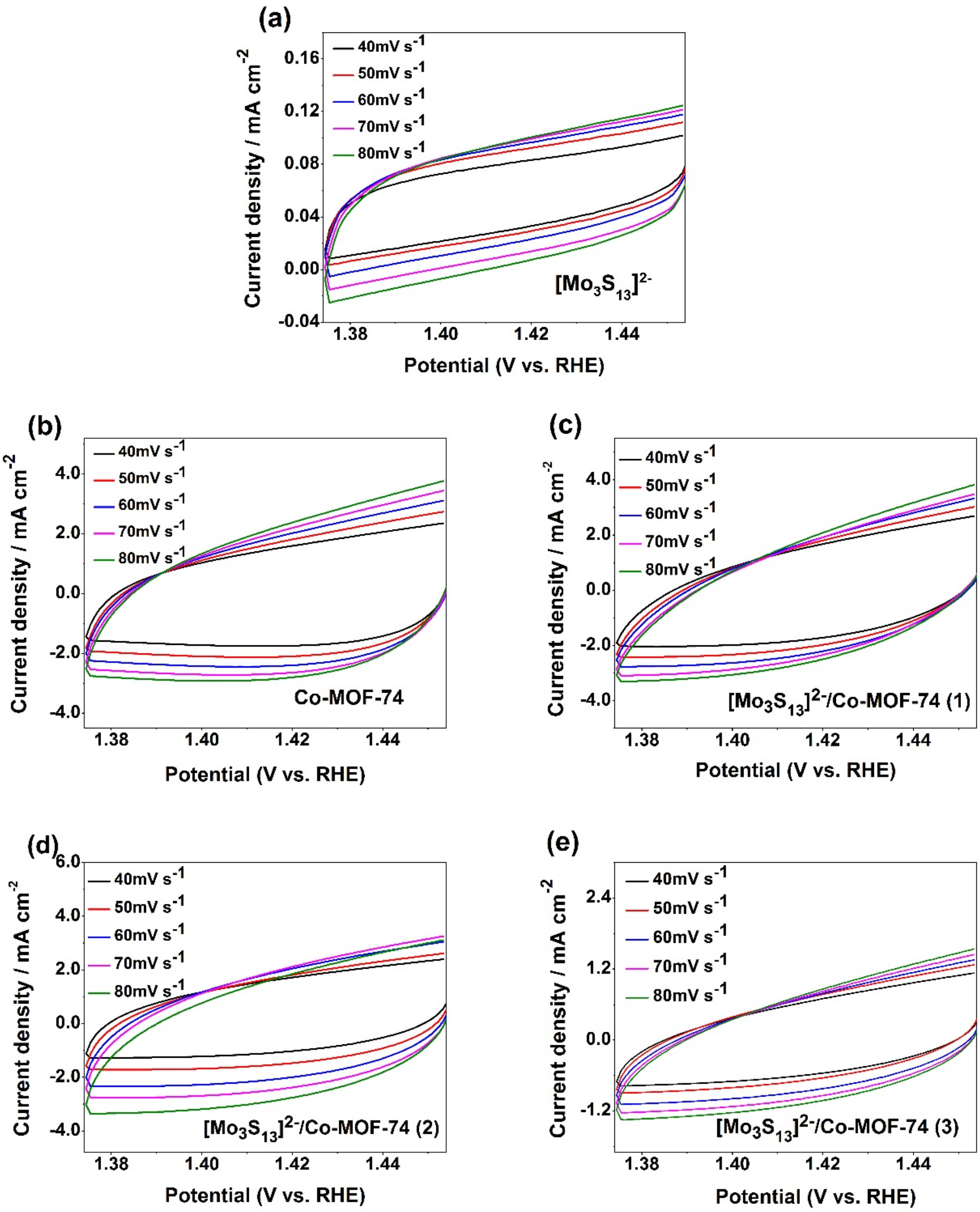

Fig. S4 The CV curves under different scan rates (40 mV/s to 80 mV/s) for $[Mo_3S_{13}]^{2-}$ (a), Co-MOF-74 (b), $[Mo_3S_{13}]^{2-}$/Co-MOF-74 **(1)** (c), $[Mo_3S_{13}]^{2-}$/Co-MOF-74 **(2)** (d) and $[Mo_3S_{13}]^{2-}$/Co-MOF-74 **(3)** (e) in 1 M KOH.

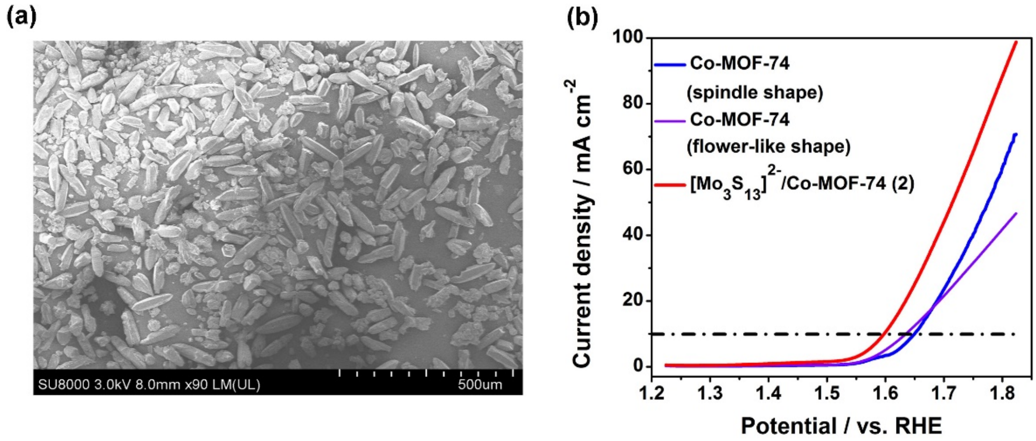

Fig. S5 (a) Scanning electron microscopy (SEM) image of Co-MOF-74 with spindle morphology. (b) LSV curves of Co-MOF-74 and $[Mo_3S_{13}]^{2-}$ /Co-MOF-74 **(2)** with different morphologies in 1 M KOH solution.

Table S1 The molar ratios of Mo and Co in different catalysts were determined by inductively coupled plasma mass spectrometry (ICP-MS).

Samples	Feeding molar ratio (Mo/Co)	Final molar ratio (Mo/Co)
Co-MOF-74	0	0
$[Mo_3S_{13}]^{2-}$/Co-MOF-74 **(1)**	0.07	0.05
$[Mo_3S_{13}]^{2}$/Co-MOF-74^{-}**(2)**	0.2	0.07
$[Mo_3S_{13}]^{2-}$/Co-MOF-74 **(3)**	0.4	0.2

Table S2 Comparison of OER catalytic performance of some reported electrocatalysts and $[Mo_3S_{13}]^{2-}$/Co-MOF -74 in alkaline solution.

Catalyst	Electrodes	Electrolyte	Over potential (10 mA/cm^2) vs. RHE (V)	Tafer slope (mV dec^{-1})	Ref.
Fe/Co NH_2BDC MOF	FTO	1M KOH	0.520	101	1
RuO_2	CP	1 M KOH	0.405	126	2
Ni BTC	CP	1 M KOH	0.346	64	2
N-doped Graphene CoO	RDE	1 M KOH	0.340	71	3
Co NPs/N-C-800	RDE	1 M KOH	0.379	61.4	4
Co-BTC	GCE	1 M KOH	0.386	84.78	5
ZIF-67@POM	GCE	1 M KOH	0.490	88	6
CoOx-ZIF	GCE	0.1M NaOH	0.318	70.3	7
Co-ZIF-9	FTO	0.1 KOH	0.510 @1mA cm^{-2}	93	8
ZIF-67@NPC-2 (2:1)	RDE	0.1 M KOH	0.410	114	9
CoP/NCNHP	GCE	1 M KOH	0.310	70	10
Mo-N/C@MoS_2	GCE	1 M KOH	0.390	72	11
NNU-23	CC	0.1 M KOH	0.365	81.8	12
$Co_6Mo_6C_2$@NCNT-800	GCE	1 M KOH	0.361	48.37	13
FeNi-MOF-74	NF (Ni foam)	1 M KOH	0.223	71.6	14
NiFc-MOF	NF	1 M KOH	0.195	44.1	15
Cu–Fe–NH_2 MOF	NF	1 M KOH	0.33 @500 mA cm^{-2}	60.8	16
NiCo-UMOFNs	GCE	1 M KOH	0.189	42	17
$[Mo_3S_{13}]^{2-}$ /Co-MOF-74 (2)	**GCE**	**1 M KOH**	**0.368**	**90.6**	**This work**

References

S1 B. Iqbal, M. Saleem, S. N. Arshad, J. Rashid, N. Hussain and M. Zaheer, *Chemistry*, 2019, **25**, 10490-10498.

S2 V. Maruthapandian, S. Kumaraguru, S. Mohan, V. Saraswathy and S. Muralidharan, *Chemelectrochem*, 2018, **5**, 2795-2807.

S3 S. Mao, Z. Wen, T. Huang, Y. Hou and J. Chen, *Energy Environ. Sci.*, 2014, **7**, 609-616.

S4 Y. Su, Y. Zhu, H. Jiang, J. Shen, X. Yang, W. Zou, J. Chen and C. Li, *Nanoscale*, 2014, **6**, 15080-15089.

S5 L. Yaqoob, T. Noor, N. Iqbal, H. Nasir, M. Sohail, N. Zaman and M. Usman, *Renew Energ*, 2020, **156**, 1040-1054.

S6 Y. Wang, Y. Y. Wang, L. Zhang, C. S. Liu and H. Pang, *Inorg. Chem. Front.*, 2019, **6**, 2514-2520.

S7 S. Dou, C. L. Dong, Z. Hu, Y. C. Huang, J. l. Chen, L. Tao, D. Yan, D. Chen, S. Shen, S. Chou and S. Wang, *Adv. Funct. Mater.*, 2017, **27**, 1702546.

S8 S. Wang, Y. Hou, S. Lin and X. Wang, *Nanoscale*, 2014, **6**, 9930-9934.

S9 H. Wang, F.-X. Yin, B.-H. Chen, X.-B. He, P.-L. Lv, C.-Y. Ye and D.-J. Liu, *Appl. Catal. B Environ.*, 2017, **205**, 55-67.

S10 Y. Pan, K. A. Sun, S. J. Liu, X. Cao, K. L. Wu, W. C. Cheong, Z. Chen, Y. Wang, Y. Li, Y. Q. Liu, D. S. Wang, Q. Peng, C. Chen and Y. D. Li, *J. Am. Chem. Soc.*, 2018, **140**, 2610-2618.

S11 I. S. Amiinu, Z. Pu, X. Liu, K. A. Owusu, H. G. R. Monestel, F. O. Boakye, H. Zhang and S. Mu, *Adv. Funct. Mater.*, 2017, **27**, 1702300.

S12 X. L. Wang, L. Z. Dong, M. Qiao, Y. J. Tang, J. Liu, Y. Li, S. L. Li, J. X. Su and Y. Q. Lan, *Angew. Chem. Int. Ed.*, 2018, **57**, 9660-9664.

S13 X. Feng, X. Bo and L. Guo, *J. Colloid Interface Sci.*, 2020, **575**, 69-77.

S14 J. Xing, K. Guo, Z. Zou, M. Cai, J. Du and C. Xu, *Chem. Commun.*, 2018, **54**, 7046-7049.

S15 J. Liang, X. Gao, B. Guo, Y. Ding, J. Yan, Z. Guo, E. C. M. Tse and J. Liu, *Angew. Chem. Int. Ed.*, 2021, **60**, 12770-12774.

S16 N. K. Shrestha, S. A. Patil, S. Cho, Y. Jo, H. Kim and H. Im, *J. Mater. Chem. A*, 2020, **8**, 24408-24418.

S17 S. Zhao, Y. Wang, J. Dong, C.-T. He, H. Yin, P. An, K. Zhao, X. Zhang, C. Gao, L. Zhang, J. Lv, J. Wang, J. Zhang, A. M. Khattak, N. A. Khan, Z. Wei, J. Zhang, S. Liu, H. Zhao and Z. Tang, *Nat. Energy*, 2016, **1**, 16184.